

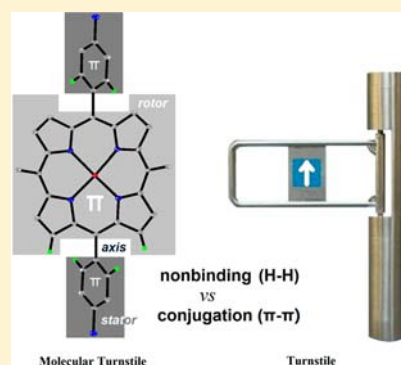
Geometry and Temperature Dependence of *meso*-Aryl Rotation in Strained Metalloporphyrins: Adjustable Turnstile Molecules

Zaichun Zhou,* Xi Zhang, Qiuhua Liu,* Ziqiang Yan, Chengjin Lv, and Ge Long

School of Chemistry and Chemical Engineering, Key Laboratory of Theoretical Chemistry and Molecular Simulation of Ministry of Education, and Hunan Provincial University Key Laboratory of QSAR/QSPR, Hunan University of Science and Technology, Xiangtan 411201, China

Supporting Information

ABSTRACT: The rotation of *meso*-aryl groups in porphyrins depends on the degree of macrocyclic distortion and is also influenced by the surrounding temperature. Dynamic NMR methods and crystal structures of series of nonplanar metalloporphyrins reveal that macrocyclic distortion lowers the rotational barrier by weakening the nonbinding interactions of neighboring groups, while increased temperature allows the rotational barrier to be overcome more readily. Two empirical methods are developed to acquire the rotational barrier. This type of strained molecule can act as an adjustable molecular turnstile through adjusting the degree of macrocyclic distortion and changing the surrounding temperature.



INTRODUCTION

Achieving specific or multifunctional properties is always one of the main goals in developing molecular devices.¹ Rotation of hindered bonds in organic molecules and biomolecules has attracted ongoing interest from many investigators.^{2–5} The rotation of substituent groups in porphyrins is a popular example because of their unique symmetry, size, and shape,⁶ and such rotation is widely used in the design of molecular devices⁷ including molecular rotor,^{8,9} molecular switches,^{10,11} molecular turnstiles,^{12,13} molecular gates,¹⁴ molecular gyroscope,¹⁵ and light-harvesting arrays.^{16–18} It has also been applied in the measurement of fluorescence anisotropy,¹⁹ construction of asymmetric molecules,²⁰ and development of long-range electronic communication.²¹

Nonbinding interactions are important in maintaining the metastability of biological macromolecules.²² The rotation of *meso*-aryl groups is a competitive consequence of a nonbinding injection in neighboring protons to the coplanarity of *meso*-aryl groups to macrocycle in porphyrin (Figure 1). The neighboring protons denote the aryl ortho protons and β -pyrrole protons closely adjacent to rotatable *meso*-position in porphyrins, the nonbinding injection will occur when the aryl group and the macrocycle are nearly coplanar.²³ While the two planes from the *meso*-aryl and macrocycle are apt to maintain coplanarity because of their conjugation feature. Therefore, changing the steric interaction between both protons should affect the rotational barriers of *meso*-aryl groups and the relative rotation rate.

An inspection of the structure of 5,15-diarylporphyrin (Figure 1) reveals that the two aryl groups are oppositely distributed on both sides of the macrocycle and adopt a cross

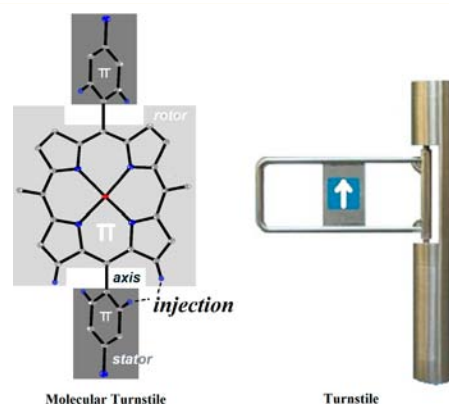


Figure 1. Schematic representation of influence factors on *meso*-aryl rotation in porphyrin and potential turnstile molecule.

arrangement to the macrocycle because of the nonbinding injection of the closest protons between aryl and pyrrole protons. If the injection were weakened, it is expected that they would tend to coplanar arrangement through the aryl rotation because of the need of their conjugation. If the both actions are weak enough and maintain an equilibrium state, a molecule rotation would achieve such that its macrocycle would be like a rotor (the aryl is hypothesized as stators), which implies the formation of a turnstile molecule.

The rotation of *meso*-aryl groups is influenced by both the macrocyclic geometry and surrounding temperature. Numerous

Received: January 17, 2013

Published: September 5, 2013

computational and experimental studies^{24,25} have explored the relationship of this rotation to structure and temperature, for example, unusual aryl-porphyrin rotational barriers are found in peripherally crowded porphyrins.^{24,25} However, no direct and quantitative relationship between these factors has been determined.

In our previous studies, we designed and synthesized several series of strapped and capped porphyrins with different deformation modes and distortion degree to explore the relationship of spectral shifts²⁶ and electron properties²⁷ to the nonplanarity of the porphyrin rings.²⁸ In these cases, we found that macrocyclic deformation can cause nonequivalence of the phenyl-*ortho* and -*meta* protons at the 10- and 20-positions because of the slight deviation of the aryl from macrocycle plane, which is helpful to quantitatively track the above relationship.

In this work, we used dynamic NMR spectroscopy (DNMR) and solid structures of series of nonplanar metalloporphyrins to demonstrate that *meso*-aryl rotation depends not only on the surrounding temperature but also on the macrocyclic deformation of the porphyrin.

RESULTS AND DISCUSSION

The series of 5,15-*meso-meso*-strapped porphyrins 1 to 5 (Figure 2-top) was selected as model compounds for this study

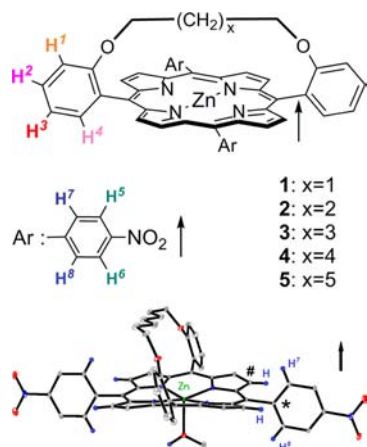


Figure 2. Structure of model compounds 1–5 (top) and the nonequivalence of the *meso*-phenyl protons according to the crystal structure of compound 5 (bottom, all protons are omitted except for the diagnostic ones). H⁵ and H⁶ and H⁷ and H⁸ become two pairs of nonequivalent protons after macrocyclic deformation.

because of their arc-type conformation^{26,27} and acquirable degree of macrocyclic distortion.²⁹ These types of strapped structures not only effectively avoid disturbances caused by substituent effects and the exchange of conformations in porphyrins with crowded peripheries that represent the most popular distorted porphyrin samples,²⁴ but also show two pairs of nonequivalent *meso*-aryl protons (H⁵ and H⁶ and H⁷ and H⁸) that act as diagnostic signals to track changes in aryl rotation (Figure 2, bottom).

The rotation of *meso*-aryl groups is strongly related to the macrocyclic distortion of porphyrin.²⁶ The ¹H NMR signals for the ortho protons of *meso*-nitrophenyl groups of compound 5 appeared at two positions (Figure 2 and 3, H⁷ and H⁸), while the same two signals averaged into one peak for compounds 1 and 2, and they partially disappeared in compounds 3 and 4 on the NMR time scale at 293 K. The NMR signals of the

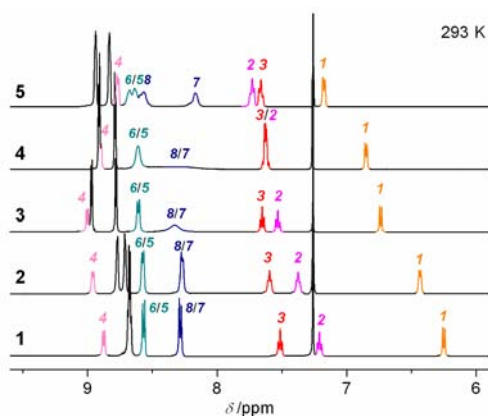


Figure 3. Changes in the ¹H NMR signals of the aromatic protons in model compounds 1–5 at 293 K in chloroform solution. The numbers labeled denote H^{1–4}, H⁷ and H⁸, or H⁵ and H⁶ described in Figure 2.

nonequivalent meta-protons (H⁵ and H⁶) showed a similar trend to those of the nonequivalent ortho protons. The lack of splitting of the ortho-protons originates from the rotation of the *meso*-substituents. This implies that deformation of the tetrapyrrole macrocycle is potentially useful to regulate rotation of the *meso*-aryl group, which drove us to explore the relationship between rotation of *meso*-aryl groups and macrocyclic deformation, as well as the coalescence temperature (T_C) of the rotation.

Changing the surrounding temperature influences the rotation (or rotation rate) of *meso*-groups in porphyrins. Dynamic NMR spectroscopy method³⁰ was used to follow the rotation in each compound. Increasing the surrounding temperature can allow the rotational barrier (ΔG^\ddagger) of *meso*-groups to be overcome. Taking a variable-temperature NMR (VT-NMR) experiment on compound 4 as an example (Figure 4), the two diagnostic signals (H⁷ and H⁸, represented by unfilled circles) gradually separated and showed an apparent AB pattern as the temperature decreased, while at elevated temperature they averaged into one signal. Another two diagnostic signals (H⁵ and H⁶, represented by arrows, see Supporting Information S14) showed the same trend as those of H⁷ and H⁸. This demonstrates that rotation of the *meso*-nitrophenyl group in compound 4 depends on the temperature, and the T_C of *meso*-group rotation is about 303 K. The rotation of the *meso*-group is generally assumed to be fast on the NMR time scale above T_C (~ 303 K) and either very slow or absent below T_C .

The rotation of *meso*-aryl groups in porphyrins relies mainly on the molecular geometry, as well as the surrounding temperature, and macrocyclic distortion is the major geometry factor. An inspection of the DNMR results of compounds 1–5 (Figure 4) showed that the diagnostic signals change in a similar manner to those of compound 4; the two diagnostic signals (H⁷ and H⁸ or H⁵ and H⁶) appeared at two isolated positions at low temperature and gradually averaged into one signal as the temperature increased. The only difference is in their T_C , with the higher the degree of macrocyclic distortion, the lower T_C .

Their coalescence temperatures (T_C) can be obtained from a plot of the signal width at half-height against the experimental temperature (T), which is convenient to quantitatively assess the relationship of *meso*-aryl rotation to macrocyclic geometry. The first rotation (possibly slow) of the *meso*-nitrophenyl

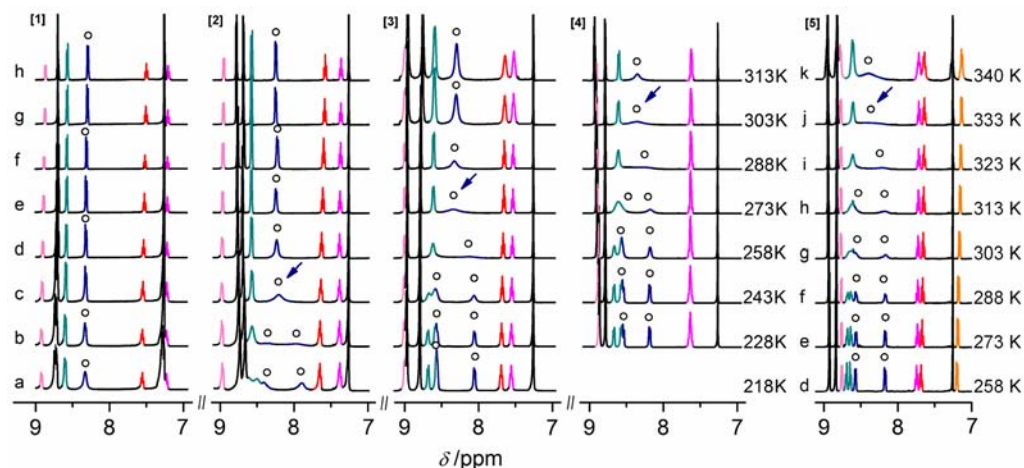


Figure 4. DNMR spectra of model compounds 1–5 obtained by VT-NMR experiments and determination of their coalescence temperatures (T_C shown by arrows); the unfilled circles represented the diagnostic signals, H^7 and H^8 described in Figure 2.

groups leads to distinct broadening of the diagnostic signals. Therefore, the T_C can be reflected in the changes of the half-height peak width (W_{hh}) of a diagnostic proton (e.g., H^7) as the determined temperature changed (Figure 5). T_C of compounds, 2, 3, 4, and 5, can easily be obtained from a plot of W_{hh} against T . And that of compound 1 can also be reasonably acquired by extension of the equivalent plot because four of the W_{hh} have a good linear correlation to their T_C (See Supporting Information S3), although it cannot be directly extracted through the

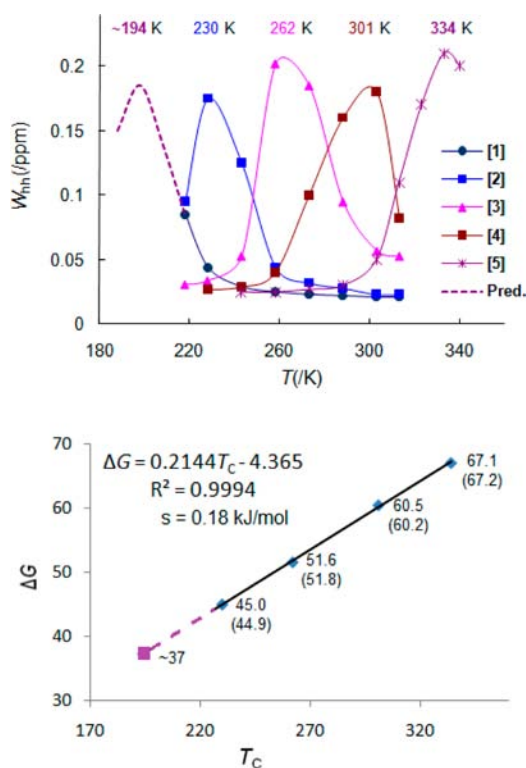


Figure 5. Plot of half-height peak width (W_{hh}) of the diagnostic proton H^7 against determined temperature (T) (top), and the relationship of rotational barrier (ΔG^\ddagger) to coalescence temperatures (T_C) (bottom) for complexes 2–5. The extended lines (dash line) are for predicting ΔG^\ddagger of compound 1 and the numbers denote ΔG^\ddagger and their relative fitted values (in brackets).

DNMR method because of the poor solubility at its T_C temperature in chloroform solution.

The out-of-plane deformability of a macrocycle is important for lowering the activation energy for rotation of *meso*-substituents on a porphyrin.^{6,7} The rotation of the *meso*-aryl units pushes neighboring protons aside to overcome nonbonding interactions.³¹ The distance (d_{HH}) between the aryl ortho protons and the porphyrin β -pyrrole protons increases when the aryl group and porphyrin are nearly coplanar because the degree of macrocyclic distortion increased, which weakens the steric interaction and lowers the rotational barrier (ΔG^\ddagger) (Figure 6).

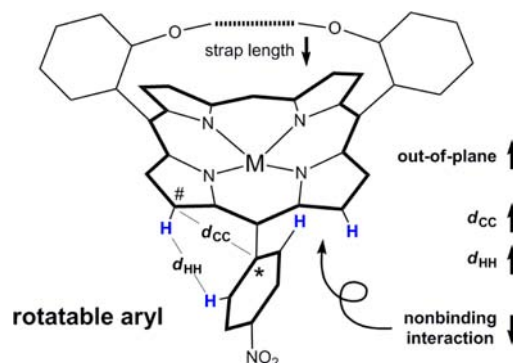


Figure 6. Schematic representation of the weakening of nonbinding interactions as the degree of macrocyclic distortion increases. M is the potential metal ions.

The rotational barrier (ΔG^\ddagger) is related to the degree of macrocyclic distortion. The rotation of *meso*-aryl groups can also be quantitatively assessed by the ΔG^\ddagger because coalescence temperature (T_C) can be used to estimate the rate of aryl rotation and the free energy. The ratio of ΔG^\ddagger to C_m-C bond was obtained using a standard equation (eq 1) for DNMR methods.^{23,32,33}

$$\frac{\Delta G^\ddagger}{RT_C} = 22.96 + \ln \frac{T_C}{\Delta\nu} \quad (1)$$

where $\Delta\nu$ is the difference in chemical shift between the exchanging signals (in Hz) extrapolated to T_C . The results of this calculation are shown in Table 1.

Table 1. Relationship of Rotation Barrier (ΔG^\ddagger) to Coalescence Temperature (T_C), the Absorptive Maxima (λ_{\max}), the Chemical Shift (δ) of Ether Protons, and the d_{CC} ^a

compd. (n_C)	1 (3)	2 (4)	3 (5)	4 (6)	5 (7)
ΔG^\ddagger (kJ·mol ⁻¹)	~37 ^a	45.0	51.6	60.5	67.1
T_C (K)	~194 ^a	230	262	301	334
$\Delta\nu$ (Hz) ^b		127.8	123.8	87.5	100.3
λ_{\max} (nm)	446.1	437.1	431.9	426.6	422.7
$\delta(\text{OCH}_2/\text{ppm})^c$	-1.00	0.39	0.85	2.06	2.84
d_{CC} (Å) ^d	2.97	2.96	2.94	2.93	2.92

^a ΔG^\ddagger and T_C value of compound **1** is acquired by extension of the plot in Figure 5. ^b $\Delta\nu$ is the difference in chemical shift between the exchanging signals. ^c $\delta(\text{OCH}_2)$ is the chemical shift of ether protons in straps. ^d d_{CC} is the averaged distance between β -carbon and aryl carbon closely adjacent to rotatable *meso*-position.

The higher the degree of macrocyclic distortion is, the lower ΔG^\ddagger is. The ΔG^\ddagger of compound **1** is only ~37 kJ/mol, the rotation of its *meso*-nitrophenyl group readily occurs at ambient or a lower temperature at this energy level. For compounds **2** and **3**, ΔG^\ddagger can also be overcome at ambient temperature. When d_{CC} decreases as for compound **5**, ΔG^\ddagger increases by ~30 kJ/mol compared to that of compound **1** to 67.1 kJ/mol. Thus, for rotation of *meso*-aryl groups to occur at this energy level, which is close to the value (~77 kJ/mol) obtained for previous regular planar porphyrins,^{24,34} the temperature needs to be greatly increased.

The distance (d_{HH}) between the aryl ortho protons and the porphyrin β -pyrrole protons is changeable and difficult to be determined, and these molecules in solution when the rotation occurs at transition state, cannot also be really reflected by their solid structure at ground state. The real value of d_{HH} is not readily acquirable at both states, but it is related to the distance of C–C (d_{CC}) which is defined as the averaged distance between β -carbon (# in Figure 6) and aryl carbon (*) closely adjacent to rotatable *meso*-position. (See Supporting Information S5–7)

For model compounds **1–5**, not enough crystal structures can be used to extract the structural parameter, d_{CC} , but the data of d_{CC} can be indirectly in analogy to strapped iron porphyrins, **1-Fe–5-Fe**, in our recent report (Figure 7)²⁷

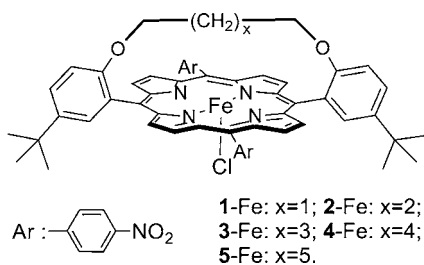


Figure 7. Strapped iron porphyrins, **1-Fe–5-Fe**.

because they have the same molecular skeleton and changing trends in structure as those of compounds **1–5** (See Supporting Information S7). The crystal structures of the compounds **1-Fe–5-Fe** revealed that their macrocycles also adopted an arc-type deformation due to the shrinkage caused by the straps and the deviation of aryl groups from macrocyclic plane became larger and larger as the straps were shortened. Furthermore, the distance, d_{CC} , continuously increases from 2.92 to 2.97 Å when n_C in straps is from 7 to 3 and therefore

weakens the nonbinding interaction of relative protons. The distance parameter, d_{CC} , for the five compounds **1-Fe–5-Fe** is shown in Table 1.

It is necessary to establish a relationship between the rotational barrier (ΔG^\ddagger) and some structure or property parameters easily acquired. The ¹H NMR and absorptive spectra were determined at the similar solution circumstance to those of acquirement of T_C (or ΔG^\ddagger). Two parameters, the chemical shift of ether protons, $\delta(\text{OCH}_2)$, and the absorptive maxima, λ_{\max} , were selected to follow the change of the barrier.

There is a good relationship of the rotational barrier (ΔG^\ddagger) to the $\delta(\text{OCH}_2)$ and an empirical equation can be fitted through a linear treatment of the both (Figure 8). The protons

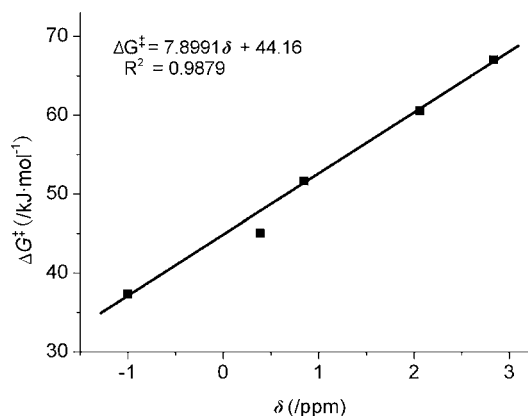


Figure 8. Plot of rotational barrier (ΔG^\ddagger) of the *meso*-aryl group to the chemical shift of ether protons, δ (OCH_2/ppm), $\delta(\text{OCH}_2)$ is described in Table 1. The inset shows an empirical equation.

will be gradually pulled into the shielding center of the macrocycle as the straps decreased, and the $\delta(\text{OCH}_2)$ will regularly shift to a higher field. In turn, the shift value will recover to the original one at low field. Another phenyl signal, H^1 , adjacent to ether displayed the same rule as those of ether protons (See Supporting Information S11).

The absorptive maxima, λ_{\max} , provides another independent avenue to track the rotational barrier (ΔG^\ddagger). Both of ΔG^\ddagger and λ_{\max} take on a main linear correlation and a slight deviation. An empirical equation can be obtained through their nonlinear fitting (Figure 9). The ΔG^\ddagger of regular planar porphyrin (e.g., 5,10,15,20-tetraphenyl porphyrin, TPP) can be predicted

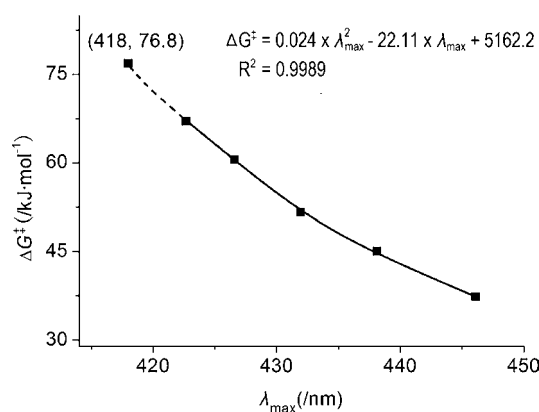


Figure 9. Plot of rotational barrier (ΔG^\ddagger) of the *meso*-aryl group to the absorptive maxima (λ_{\max}). λ_{\max} is described in Table 1.

according to the equation, and the value calculated is 76.8 kJ/mol ($\lambda_{\text{max}}(\text{TPP}) = 418 \text{ nm}$) which is in line with the results, $\sim 77 \text{ kJ/mol}$, from literature.^{24,34}

The fitting curve displays a tiny deviation from linear feature. It was thought that the macrocyclic distortion of model compounds includes the out-of-plane deformation and the in-plane one, and the absorptive red-shift is derived from out-of-plane feature.²⁶ While the in-plane deformation along the direction of two ethers in straps will become visible as the distortion degree increase, the blue-shift from in-plane deformation will slightly offset the red-shift from out-of-plane one. That is, the in-plane deformation possibly results in the tiny deviation.

It should be noted that aryl rotation barrier, ΔG^\ddagger , in a regular porphyrin is difficult to exceed the value, $\sim 77 \text{ kJ/mol}$ (that is, 18.4 kcal/mol)²⁴ even though the porphyrin can readily assume planarity. This is because of the out-of-plane flexibility of the porphyrin macrocycle.³⁵ Many factors influence the non-planarity of the macrocycle to a small degree, for example, solvent effects, central metal complexation^{6,23} and axial coordination.²⁴ These factors can slightly lower the ΔG^\ddagger for *meso*-aryl rotation.

CONCLUSION

It is found that *meso*-aryl rotation in porphyrins mainly depends on the degree of macrocyclic distortion as well as the surrounding temperature. Macrocyclic distortion causes neighboring protons to move apart and lowers the rotational barrier of the *meso*-group, the difference in free energies between the transition state of sample and its ground state. Two empirical methods are developed to acquire the rotational barrier by applying the good relationship of the barrier to the chemical shift of diagnostic protons or the absorptive maxima. This type of strained molecule can act as an adjustable molecular turnstile through adjusting the degree of macrocyclic distortion and changing the surrounding temperature. Our findings may provide insight for the design of molecular devices.

EXPERIMENTAL SECTION

Preparation of Model Compounds. The target nonplanar zinc porphyrins 1–5 and iron complexes 1-Fe–5-Fe were prepared according to our previous reports,^{26,27} and their crystals were obtained through solvent diffusion method in chloroform and methanol.

ASSOCIATED CONTENT

Supporting Information

Experimental procedures and DNMR of compounds. This material is available free of charge via the Internet at <http://pubs.acs.org>.

AUTHOR INFORMATION

Corresponding Authors

*E-mail: zhouzaichun@hnust.edu.cn (Z.Z.).

*E-mail: liuqiuhua@hnust.edu.cn (Q.L.).

Notes

The authors declare no competing financial interest.

ACKNOWLEDGMENTS

The help of Prof. Jianyu Zheng of Nankai University and Dr. Xianyong Yu of Hunan University of Science and Technology is acknowledged. This work was supported by the National

Natural Science Foundation of China (No. 21071051), the Key Project of the Chinese Ministry of Education (No. 211121), and the Scientific Research Fund of Hunan Provincial Education Department (No: 10B031).

REFERENCES

- Balzani, V.; Credi, A.; Raymo, F. M.; Stoddart, J. F. *Angew. Chem., Int. Ed.* **2000**, *39*, 3348.
- Dugave, C.; Demange, L. *Chem. Rev.* **2003**, *103*, 2475.
- Skopek, K.; Hershberger, M. C.; Gladysz, J. A. *Coord. Chem. Rev.* **2007**, *251*, 1723.
- Garcia-Garibay, M. A. *Proc. Natl. Acad. Sci. U. S. A.* **2005**, *102*, 10771.
- Couzijn, E. P. A.; Slootweg, J. C.; Ehlers, A. W.; Lammertsma, K. *J. Am. Chem. Soc.* **2010**, *132*, 18127.
- (a) Yatsunyk, L. A.; Shokhirev, N. V.; Walker, F. A. *Inorg. Chem.* **2005**, *44*, 2867. (b) Yatsunyk, L. A.; Ogura, H.; Walker, F. A. *Inorg. Chem.* **2005**, *44*, 2848.
- Balzani, V.; Venturi, M.; Credi, A. *Molecular Devices and Machines: A Journey into the Nanoworld*; Wiley-VCH Verlag GmbH: Weinheim, Germany, 2003.
- Écija, D.; Auwärter, W.; Vijayaraghavan, S.; Seufert, K.; Bischoff, F.; Tashiro, K.; Barth, J. V. *Angew. Chem., Int. Ed.* **2011**, *50*, 3872; *Angew. Chem.* **2011**, *123*, 3958.
- Ikeda, M.; Takeuchi, M.; Shinkai, S.; Tani, F.; Naruta, Y.; Sakamoto, S.; Yamaguchi, K. *Chem.—Eur. J.* **2002**, *8*, 5541.
- Zhou, Z. C.; Cao, C. Z.; Yin, Z. Q.; Liu, Q. H. *Org. Lett.* **2009**, *11*, 1781.
- Zhou, Z. C.; Yang, Y.; Zhu, Y. Z.; Zheng, J. Y. *Chin. J. Chem.* **2008**, *26*, 1913.
- Guenet, A.; Graf, E.; Kyritsakas, N.; Hosseini, M. W. *Chem.—Eur. J.* **2011**, *17*, 6443.
- Lang, T.; Graf, E.; Kyritsakas, N.; Hosseini, M. W. *Chem.—Eur. J.* **2012**, *18*, 10419.
- Guenet, A.; Graf, E.; Kyritsakas, N.; Hosseini, M. W. *Inorg. Chem.* **2010**, *49*, 1872.
- Boitrel, B.; Lecas, A.; Renko, Z.; Rose, E. *J. Chem. Soc., Chem. Commun.* **1985**, 1820.
- Li, F. R.; Yang, S. I.; Ciringh, Y.; Seth, J.; Martin, C. H., III; Singh, D. L.; Kim, D.; Birge, R. R.; Bocian, D. F.; Holten, D.; Lindsey, J. S. *J. Am. Chem. Soc.* **1998**, *120*, 10001.
- McDermott, G.; Prince, S. M.; Freer, A. A.; Hawthornthwaite-Lawless, A. M.; Papiz, M. Z.; Cogdell, R. J.; Isaacs, N. W. *Nature* **1995**, *374*, 517.
- Karrasch, S.; Bullough, P. A.; Ghosh, R. *EMBO J.* **1995**, *14*, 631.
- Cho, H. S.; Rhee, H.; Song, J. K.; Min, C. K.; Takase, M.; Aratani, N.; Cho, S.; Osuka, A.; Joo, T.; Kim, D. *J. Am. Chem. Soc.* **2003**, *125*, 5849.
- Bringmann, G.; Götz, D. C. G.; Gulder, T. A. M.; Gehrke, T. H.; Bruhn, T.; Kupfer, T.; Radacki, K.; Braunschweig, H.; Heckmann, A.; Lambert, C. *J. Am. Chem. Soc.* **2008**, *130*, 17812.
- Nemykin, V. N.; Rohde, G. T.; Barrett, C. D.; Hadt, R. G.; Sabin, J. R.; Reina, G.; Galloni, P.; Floris, B. *Inorg. Chem.* **2010**, *49*, 7497.
- Bäckström, A.; Lundberg, C.; Kersulyte, D.; Berg, D. E.; Borén, T.; Arqvist, A. *Proc. Natl. Acad. Sci. U. S. A.* **2004**, *101*, 16923.
- (a) Eaton, S. S.; Eaton, G. R. *J. Chem. Soc., Chem. Commun.* **1974**, 605, 576. (b) Eaton, S. S.; Eaton, G. R. *J. Am. Chem. Soc.* **1975**, *97*, 3660. (c) Eaton, S. S.; Eaton, G. R. *J. Am. Chem. Soc.* **1977**, *99*, 6594.
- Medforth, C. J.; Haddad, R. E.; Muzzi, C. M.; Dooley, N. R.; Jaquinod, L.; Shyr, D. C.; Nurco, D. J.; Olmstead, M. M.; Smith, K. M.; Ma, J. G.; Shelnut, J. A. *Inorg. Chem.* **2003**, *42*, 2227.
- Nakamura, M.; Yamaguchi, T.; Ohgo, Y. *Inorg. Chem.* **1999**, *38*, 3126.
- Zhou, Z. C.; Cao, C. Z.; Liu, Q. H.; Jiang, R. Q. *Org. Lett.* **2010**, *12*, 1780.

- (27) Zhou, Z. C.; Liu, Q. H.; Yan, Z. Q.; Long, G.; Zhang, X.; Cao, C. Z.; Jiang, R. Q. *Org. Lett.* **2013**, *15*, 606.
- (28) Zhou, Z. C.; Shen, M.; Cao, C. Z.; Liu, Q. H.; Yan, Z. Q. *Chem.—Eur. J.* **2012**, *18*, 7675.
- (29) Shelnutt, J. A.; Song, X. Z.; Ma, J. G.; Jia, S. L.; Jentzen, W.; Medforth, C. J. *Chem. Soc. Rev.* **1998**, *27*, 31.
- (30) Bushweller, C. H.; Wang, C. Y.; Reny, J.; Lourandos, M. Z. *J. Am. Chem. Soc.* **1977**, *99*, 3938.
- (31) Moigne, C. L.; Picaud, T.; Boussac, A.; Looock, B.; Momenteau, M.; Desbois, A. *Inorg. Chem.* **2003**, *42*, 6081.
- (32) Oki, M. *Applications of Dynamic NMR Spectroscopy to Organic Chemistry*; VCH: Deerfield Beach, FL, 1985.
- (33) Dirks, J. W.; Underwood, G.; Matheson, J. C.; Gust, D. *J. Org. Chem.* **1979**, *44*, 2551.
- (34) Stolzenberg, A. M.; Haymond, G. S. *Inorg. Chem.* **2002**, *41*, 300.
- (35) Cheng, R. J.; Chen, P. Y.; Gau, P. R.; Chen, C. C.; Peng, S. M. *J. Am. Chem. Soc.* **1997**, *119*, 2563.